On the Stator of Rotary ATP Synthase: The Binding Strength of Subunit δ to $(\alpha\beta)_3$ As Determined by Fluorescence Correlation Spectroscopy†

Katrin Häsler, Oliver Pänke, and Wolfgang Junge*

Department of Biology/Chemistry, Division of Biophysics, Universität Osnabrück, D-49069 Osnabrück, Germany

Received June 1, 1999; Revised Manuscript Received July 20, 1999

ABSTRACT: ATP synthase is conceived as a rotary enzyme. Proton flow drives the rotor (namely, subunits $\mathbf{c}_{12}\epsilon\gamma$) relative to the stator (namely, subunits $\mathbf{ab}_2\delta(\alpha\beta)_3$) and extrudes spontaneously formed ATP from three symmetrically arranged binding sites on $(\alpha\beta)_3$ into the solution. We asked whether the binding of subunit δ to $(\alpha\beta)_3$ is of sufficient strength to hold against the elastic strain, which is generated during the operation of this enzyme. According to current estimates, the elastically stored energy is about 50 kJ/mol. Subunit δ was specifically labeled without impairing its function. Its association with solubilized $(\alpha\beta)_3\gamma$ in detergent-free buffer was studied by fluorescence correlation spectroscopy (FCS). A very strong tendency of δ to dimerize in detergent-free buffer was apparent ($K_d \leq 0.2$ nM). Taking the upper limit of this figure into account, the dissociation constant between monomeric δ and $(\alpha\beta)_3\gamma$ was 0.8 nM if not smaller. It is equivalent to a free energy of binding of at least 52 kJ/mol and therewith is sufficient for the assumed hold-function of δ in the stator. Our data were compatible with a single binding site for δ on the hexagon of $(\alpha\beta)_3$.

ATP synthase uses proton-motive force (*1*) or sodium-motive force (*2*) across the respective coupling membrane in bacteria, mitochondria, and chloroplasts to drive the synthesis of ATP from ADP and inorganic phosphate. The catalytic headpiece, F_1, has a subunit structure of $(\alpha\beta)_3\gamma\delta\epsilon$, and the ion-translocating membrane portion, F_o, has a subunit structure of $\mathbf{ab}_2\mathbf{c}_{12}$. ATP synthase is conceived as a molecular engine (*3*−*5*). The hydrolysis of ATP drives the rotation of γ relative to the hexagonally arranged large subunits, $(\alpha\beta)_3$, in the isolated headpiece, F_1. This has been established experimentally by chemical cross-linking (*6*), by polarized absorption recovery after photobleaching (*7*), and by video microfluorometry (*8*). The rotation progresses in three steps of 120° (*9*, *10*). Cross-linking experiments have suggested that subunit γ also rotates in the holoenzyme (*11*). How torque is generated by the translocation of protons through F_o is a key question. Models have been presented in which proton translocation is mediated by a ring of 12 copies of subunit **c** that rotates relative to the larger subunit **a** of F_o (*12*−*15*) (see ref *16* for an overview). The rotation is supposedly picked up by subunits γ and ϵ and transmitted by γ into F_1. As a prerequisite for torque transmission from F_o into F_1, the hexagon of subunits $(\alpha\beta)_3$ has to be firmly linked to the stator elements of F_o. Cross-linking experiments from various laboratories (*17*−*19*) as well as the demonstration that both ϵ and γ rotate (*9*, *20*) have led to the following assignment of subunits to the rotor, namely, $\mathbf{c}_{12}\epsilon\gamma$, and the stator, namely, $\mathbf{ab}_2\delta(\alpha\beta)_3$ (reviewed in refs *5* and *21*). Figure 1 shows a model structure that has been based on structural and biochemical evidence from several laboratories as detailed in ref *21*. Cross-linking studies with engineered subunit δ have revealed that the major portion of δ is located on the outside of the upper half of F_1. The covalent

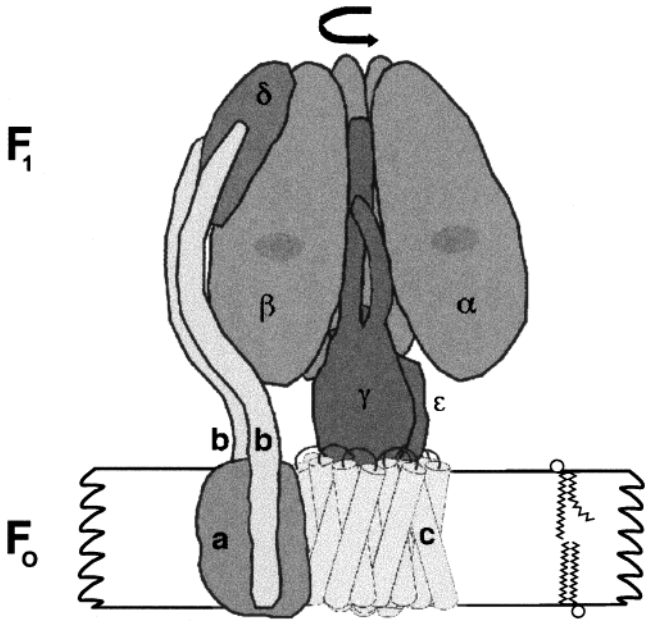

FIGURE 1: Front view of a model for F_1F_o according to ref *5*. One copy each of subunits α and β were removed to display the central shaft, subunit γ. Subunit δ is located at the outside of the upper half of F_1, and it connects the $(\alpha\beta)_3$ portion through $\mathbf{b}_2$ with **a** of the membrane-embedded F_o portion to form a stator relative to the rotor, $\mathbf{c}_{12}\epsilon\gamma$.

† This work was financially supported by the Deutsche Forschungsgemeinschaft (SFB 171−SFB 431), the HFSP-Organisation (RG15/1998-M), the Fonds der Chemischen Industrie, and the Land Niedersachsen.

* Corresponding author. Tel: +49-541-969 2872. Fax: +49-541-969 1221. E-mail: junge@uni-osnabrueck.de.

[1] Abbrevations: AC, *N*-acetylcysteine; DTT, dithiothreitol; FCS, fluorescence correlation spectroscopy; K_d, dissociation constant; mega-9, nonanoyl-*N*-methylglucamide; TMR-5-M, tetramethylrhodamin-5-maleimide.

10.1021/bi991236m CCC: $18.00
Published on Web 09/23/1999

attachment of this subunit to $(\alpha\beta)_3$ by bifunctional and photolabile cross-linkers does not inhibit the chloroplast enzyme (*17, 18*). Zero-length cross-links have been found between δ and subunit **b** (*22*), and the construction of functional chimeric enzymes requires that δ and **b** are derived from the same organism (*23*). These results have established δ as an element of the second stalk or stator running from $(\alpha\beta)_3$ via δ and $\mathbf{b}_2$ down to subunit **a** within F_o (*24, 25*) as illustrated in Figure 1. First direct evidence for the existence of at least one second stalk has recently been presented by electron microscopy (*26, 27*).

The parallelogram of two **b** subunits that are clamped by δ on the one end and by subunit **a** on the other one could serve as one elastic element (*5*) to transiently store free energy gained from the translocation of the first to the fourth proton (*28, 29*) until the reaction proceeds from one to the next out of three reaction sites on F_1. For such a function, the binding of δ to $(\alpha\beta)_3$ has to be strong enough to hold δ fast on $(\alpha\beta)_3$ against the generated torque. The binding of δ to $CF_1(-\delta,\epsilon)$ was previously assessed in our laboratory by the rotational diffusion of labeled δ in the presence/absence of $CF_1(-\delta,\epsilon)$. It yielded a rather high dissociation constant of $K_d = 100$ nM (*30*). The standard free energy of dissociation, $\Delta G° = -RT \ln K_d = 39.9$ kJ mol^{-1}, is difficult to reconcile with the free energy of elastic deformation in the three stepped progress (*9, 10*) of ATP synthesis. The binding strength has to cope with the energy equivalent to the torque, 40 pN nm (*8, 10*) times the angular displacement, namely 120°, which gives 50.5 kJ mol^{-1}.

We applied fluorescence correlation spectroscopy (FCS) for highly sensitive measurements of the concentration and diffusion time of labeled protein in dilute solution (nM range). Using TMR-labeled δ, we found that subunit δ has a strong tendency to dimerize in solution ($K_d \leq 0.2$ nM). The dimerization complicated the assessment of the binding of monomeric δ to $(\alpha\beta)_3$. Correcting for this property, we found that monomeric δ bound more strongly to $CF_1(-\delta,\epsilon)$ than previously thought. The dissociation constant was at most 0.8 nM, if not much smaller, which corresponds to $\Delta G° \geq 52$ kJ mol^{-1}.

MATERIALS AND METHODS

Preparation and Labeling of Proteins. CF_1 lacking subunits δ and ϵ ($CF_1(-\delta,\epsilon)$) was prepared by anion exchange chromatography (*31*) starting from complete spinach-CF_1 (*32*). The specific activity of the enzyme was 23 U/mg (in 50 mM Tris-HCl, pH 7.8, 5 mM ATP, 2 mM $MgCl_2$, 20% (v/v) methanol, and 10 mM Na_2SO_3, with run time 5 min at room temperature). The protein was stored as $(NH_4)_2SO_4$ precipitate at +4 °C. Prior to FCS measurements, it was desalted by gel filtration (Pharmacia NAP5, 25 mM Tris-HCl, pH 7.8).

Aliquots of complete, i.e., δ and ϵ containing CF_1 (about 1 mg/mL), were incubated for 4 h with 50 μM TMR-5-M (20 mM MOPS/NaOH, pH 7). The reaction was stopped by addition of 1 mM *N*-acetylcysteine, and free dye was removed by gel filtration (NAP10-columns, 25 mM Tris HCl, pH 7.8; $CF_1(-\delta,\epsilon)^{TMR}$ in the following). In these samples, the maleimide function was predominantly bound to the penultimate residue at the C-terminus of subunit γ (*7*).

Recombinant subunits δ_{WT} and δ_{S10C} were overexpressed in *Escherichia coli* (*33*) and purified (*18*). Prior to labeling of δ_{S10C}, DTT was removed from the samples by gel filtration (Pharmacia NAP5, 20 mM MOPS/NaOH, pH 7). The engineered cysteine residue 10 was covalently labeled with TMR-5-M (about 0.4 mg/mL protein was incubated with 200 μM TMR-5-M for 4 h at pH 7 in the dark; δ^{TMR} in the following) and the reaction stopped by addition of 1 mM *N*-acetylcysteine. Free dye, i.e., TMR-5-M covalently bound to *N*-acetylcysteine (TMR-AC), was separated from labeled protein by gel filtration (Pharmacia NAP5, 25 mM Tris-HCl, pH 7.8). The TMR/δ_{S10C} ratio in a labeled sample was adjusted to about 0.8. The protein concentration was determined according to Sedmark and Grossberg (*34*), and the one of TMR was determined by absorption at 541 nm ($\epsilon_{541} = 91000$ L mol^{-1} cm^{-1}). $\delta_{S10C}{}^{TMR}$ was stable over several months when stored in liquid nitrogen. After being thawed, samples of $\delta_{S10C}{}^{TMR}$ were analyzed by fluorescence correlation spectroscopy. According to autocorrelation analysis, a small fraction of the total dye contents (less than 20%) showed the short diffusion time of the free dye (about 54 μs in Tris buffer), and the major fraction showed the one of protein-bound dye (about 230 μs in Tris buffer). The ATPase activity of the assembled $CF_1(-\delta,\epsilon)\delta_{S10C}{}^{TMR}$ was the same as of $CF_1(-\delta,\epsilon)$ (see above) (*18*).

Fluorescence Correlation Spectroscopy. The confocal microscope 'ConfoCor' (Carl Zeiss, Jena−Evotec Biosystems, Hamburg, Germany) was used for fluorescence correlation spectroscopy (FCS) (*35*). The method is based on Brownian concentration fluctuations of fluorescent molecules in the very small volume of a laser focus ($<10^{-15}$ L) in dilute solution (<100 nM). The observed showers of fluorescence photons were submitted to autocorrelation analysis using the algorithms, hardware, and software by Evotec Biosystems (Hamburg, Germany). The autocorrelation function $g(t)$ is given by

$$g(t) = 1 + \frac{1}{N}\left(\frac{1}{\left(1+\frac{t}{\tau}\right)\sqrt{1+\frac{t}{SP^2\tau}}}\right) \quad (1)$$

where N denotes the averaged number of independently diffusing and labeled particles in the focal volume; τ is the diffusion time (see eq 2); t is the autocorrelation time; and SP is the structural parameter, which is the ratio between the long (ω_2) and the short (ω_1) axes of the focal volume. The magnitude of the autocorrelation function at time zero is reciprocally related to the average particle number in the focus, N (*36, 37*).

If the focal volume is a prolate ellipsoid of revolution with $\omega_2 \gg \omega_1$, the diffusion time can be approximated by

$$\tau \cong \frac{\omega_1^{\,2}}{4D}, \text{ in case of a sphere } D = D_{sphere} = \frac{kT}{6\pi\eta R} \quad (2)$$

where D denotes the diffusion coefficient, R is the radius of a sphere, η is the medium viscosity, k is the Boltzmann constant, and T is the temperature, as usual. The diffusion time, τ, is reciprocal to the diffusion coefficient. For spherical particles, it is reciprocal to the cubic root of the molecular weight of the labeled molecule. Figure 2 shows samples of autocorrelation functions as functions of time. They yielded the diffusion time, τ, broadly speaking the time at the point of inflection and the mean particle number, N, taken from

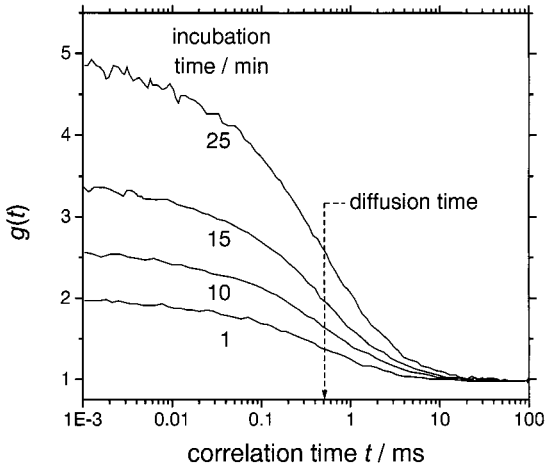

FIGURE 2: Autocorrelation functions, $g(t)$, for CF_1^{TMR} in Tris buffer as a function of the correlation time at 1, 10, 15, and 25 min after filling of the cuvette with 30 nM CF_1^{TMR}. The sampling period for each trace was 60 s. The increase of $g(t)$ reflects the unspecific adsorption of CF_1^{TMR} to the 'unblocked' chamber walls (see eq 1).

$g(t = 0)$. The curve parameter was the incubation time; the magnitude of the autocorrelation function at time zero changed because of unspecific adsorption of labeled molecules at the glass water interface (but see below).

Equations 1 and 2 hold for a pure and monodisperse solution of a single fluorescent species. A mixture of aggregates or of different types of labeled molecules produces a multi-waved shape of the autocorrelation function. It yields a spectrum of diffusion times and respective particle numbers. This was used to discriminate between monomers and dimers in pure solution of labeled δ and of free δ versus $CF_1(-\delta,\epsilon)\delta$, respectively.

For a quantitative analysis, the size and the ellipticity of the focal volume were calibrated for any solvent by a monodisperse solution of a standard dye. We used a dye with known diffusion coefficient, rhodamin-6G ($D = 2.8 \times 10^{-10}$ m^2 s^{-1}). For recalibration of the geometrical and optical parameters prior to each set of experiments in a given solvent, we used TMR-AC as a reference dye.

FCS signals were recorded in 25 mM Tris-HCl, pH 7.8, with the fluorophor concentration varying between 1 and 100 nM. The detergent mega-9 was added to the buffer in a concentration of 25 mM when indicated in the tables. Experiments with unlabeled δ were performed in the presence of 10 mM DTT. Photon showers of free dye (TMR-AC) were recorded over 20 s, and those of labeled protein were recorded over 60 s. The light output of the exciting laser (10 mW) was attenuated 10-fold to yield a mean count rate (per dye molecule in the focus) of about 30 kHz. The samples were filled into sterile tissue chambers (Nunc Lab-Tek TC Chamber Slides) built on glass cover slides (about 0.11−0.15 mm thickness).

The concentration of free dye and TMR-labeled protein was calculated from the particle number, N_i, of the respective component in FCS according to

$$c_i = \frac{N_i}{N_A V} \tag{3}$$

with V as the focal volume and the N_A as Avogadro's number.

Measurement of Viscosity and Refractive Index. The dynamic viscosity of the buffers used for FCS measurements was determined in an Ubbelohde viscosimeter (Schott). The viscosity, η, was calculated from the flow time, t, according to $\eta = kt\rho$, where ρ denotes the density of the fluid and $k = 0.01014$, an instrument-specific constant. The refractive index of buffers was determined in a refractometer (type 10460, Reichert).

RESULTS

Adsorption of Dye and Protein to the Cuvette. In a first set of experiments, we assayed the transient instability of a solution of CF_1^{TMR} that might be caused by unspecific adsorption at the glass/buffer and buffer/air interfaces and by self-aggregation: Figure 2 shows a series of autocorrelation functions that were recorded with a solution of CF_1^{TMR} with an initial protein concentration of 30 nM. The respective curves were sampled at 1, 10, 15, and 25 min after filling of the cuvette. The extent of the autocorrelation function at time zero increased over the sampling time. It revealed that the number of freely diffusing particles in the laser focus *decreased* over the incubation time (see eq 1) because of the adsorption of fluorophor-labeled protein to surfaces. The diffusion time, τ, on the other hand (namely, 500 μs), remained constant over time. Accordingly, there was no self-aggregation of CF_1^{TMR} over this time interval. To minimize the adsorption, the chamber slides were incubated with 1% blocking reagent (casein, Boehringer Mannheim) in 25 mM Tris-HCl, pH 7.8, for 2 h; washed with demineralized water; and dried prior to FCS measurements. After this treatment, unspecific adsorption was no longer detected.

Characterization of δ^{TMR} in Solution. The concentration of free dye and δ^{TMR} in 25 mM Tris-HCl, pH 7.8, was determinated by FCS. Surprisingly, the particle number of δ^{TMR} was about 2-fold lower than expected, based on the added amounts of this solute. In line with this observation, the diffusion time was longer than expected. Both indicated a strong tendency of δ to dimerize. As a test for aggregation, comparative measurements were carried out with and without addition of 25 mM detergent mega-9. We expected that a possible aggregation was prevented by the detergent when added above the critical micellar concentration. The results are presented in Table 1.

(a) Effect of Mega-9 on the Viscosity and the Refractive Index. The mean particle number, N, and the diffusion time, τ, as determined by FCS depend on the size of the focal volume element. This volume is determined by the optical parameters, namely, the refractive indices of the solution, of the glass, and of the index-matching fluid. The diffusion time, τ, also depends on the viscosity of the buffer. What was the effect of 25 mM mega-9 on the viscosity and the refractive index? Upon the addition of mega-9 to Tris buffer, both parameters were only very slightly altered (see Table 2). The change of the viscosity was much smaller (4%) as compared with the observed change of the diffusion time (about 30%). As the diffusion time is proportional to the viscosity (eq 2), the observed decrease of the particle number was not mainly attributable to this particular parameter but rather to the increased focal volume, which was due to the changed index of refraction in the presence of mega-9. This

Table 1: Calculated Free Particle Concentration of the Dye TMR-AC and of δ^{TMR} in Two Buffers That Was Based on Fluorescence Correlation Spectroscopy (FCS)[a]

substance	predetermined concn (nM)	mega-9	N	τ/μs	calculated concn(nM)
TMR-AC	1	−	0.31	53.4	1.08
		+	0.43	66.7	1.26
TMR-AC	2.4	−	0.72	54.2	2.36
		+	0.99	80.6	2.46
$\delta_{S10C}{}^{TMR}$	2.4	−	0.54	226.8	1.44
		+	1.02	242.6	2.84

[a] When analyzing the data, the different focal volumes in both buffers were taken into account. The given figures for the particle number, N, and the diffusion time, τ, are the mean of 250 FCS recordings. The second column gives the respective "real concentration" as determined by absorption and protein assay, respectively. The data in the last two rows revealed that δ^{TMR} dimerized in 25 mM Tris buffer without added detergent. Contrastingly, the apparent concentration of δ^{TMR} matched the predetermined concentration in the presence of mega-9, indicating monomerization.

Table 2: Specific Viscosities and Refractive Indices of the Buffers Used for FCS Measurements As Compared with the Respective Figures for Pure Water[a]

	viscosity η (g cm^{-1} s^{-1})	Refractive Index, n
Tris	0.76	1.3330
Tris/mega-9	0.79	1.3339

[a] The data were obtained at 22 °C.

was corroborated in experiments with free and monodisperse dye with and without added mega-9. They revealed that the magnitude of the focal volume changed by about 30% (not shown).

(b) Dimerization of δ^{TMR} in Solution. The origin of the focal volume change was the slight difference of the refractive index with and without mega-9. In the further analysis of the data, the volume change was taken into account, whereas the slight effect on the viscosity was ignored. For each solvent and each single set of experiments, the focal volume was newly determined using free dye. The results were used to interpret the FCS data with labeled protein. Applying this improved procedure, the protein concentration as determinated by FCS revealed that the TMR concentration matched the expected concentration in both buffers. Contrastingly, the δ^{TMR} concentration matched the expected concentration only in the presence of mega-9. Without detergent, it was only half of that value. We concluded that δ^{TMR} dimerized when suspended in 25 mM Tris buffer without added detergent. Figure 3 shows the apparent total concentration of δ^{TMR} from FCS measurements ($[\delta]_{app} = [\delta_2] + [\delta]$) as a function of the given protein concentration. Taking into account the balance equation, $[\delta]_\Sigma = 2 \times [\delta_2] + [\delta]$, and the law of mass action, $K_d = [\delta]^2/[\delta_2]$, the apparent concentration, $[\delta]_{app}$, is calculated from

$$[\delta]_{app} = \frac{1}{2}\left([\delta]_\Sigma - \frac{K_d}{4} + \sqrt{\frac{K_d^2}{16} + \frac{K_d[\delta]_\Sigma}{2}}\right) \qquad (4)$$

A fit of the experimental data by eq 4 yielded an upper limit of the dissociation constant for the homodimer of δ, $K_d = 0.2$ nM. The true dissociation constant is probably smaller.

Binding of δ^{TMR} and $CF_1(-\delta,\epsilon)$. The binding of δ^{TMR} to $CF_1(-\delta,\epsilon)$ was studied by varying the $CF_1(-\delta,\epsilon)$ concentration at a constant δ^{TMR} concentration of 10 nM. The fit of one set of autocorrelation signals is given in Table 3. In the presence of a large excess of $CF_1(-\delta,\epsilon)$, the apparent concentration (by FCS) of δ^{TMR} (bound and unbound δ) matched the added amount. It dropped to approximately one-half of the given amount in the presence of stoichiometric $CF_1(-\delta,\epsilon)$ concentrations. This implied that monomeric δ^{TMR} bound to $CF_1(-\delta,\epsilon)$ whereas unbound δ^{TMR} dimerized. Thus, the dissociation constant of the reaction could not be determined by simply using the law of mass action as done above.

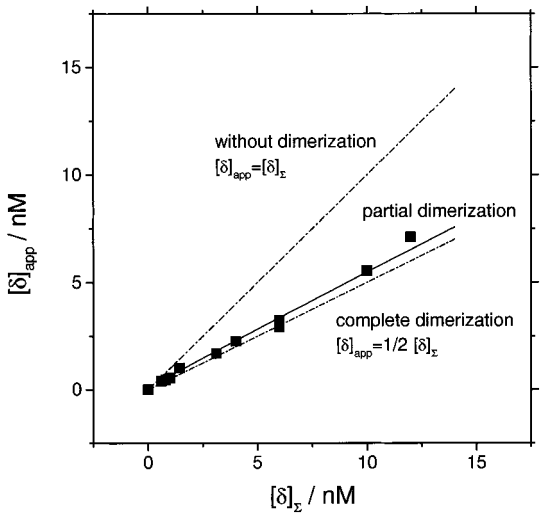

FIGURE 3: Apparent concentration by FCS of the δ subunit ($[\delta]_{app} = [\delta_2] + [\delta]$) in pure Tris buffer (pH 7.8) as derived as a function of the added concentration of δ named δ_Σ (squares, experimental; curves calculated according to eq 4).

Figure 4 shows the concentration of the formed complex $CF_1(-\delta,\epsilon)\delta^{TMR}$ as a function of the added $CF_1(-\delta,\epsilon)$ concentration. To determine the dissociation constant of the complex, we applied the model of two competitive equilibria: (a) the dimerization of δ^{TMR}, $\delta_2 \rightleftharpoons \delta + \delta$, with $K_{d,1} = 0.2$ nM, and (b) the binding of monomeric δ to $CF_1(-\delta,\epsilon)$, $CF_1(-\delta,\epsilon)\delta \rightleftharpoons \delta + CF_1(-\delta,\epsilon)$, with $K_{d,2}$. Taking into account both balance equations and the laws of mass action, the concentration of free δ^{TMR} can be calculated by finding the positive and rational root of

$$0 = [\delta]_{free} + 2\frac{[\delta]_{free}^2}{K_{d,1}} + [CF_1]_\Sigma\frac{[\delta]_{free}}{[\delta]_{free} + K_{d,2}} - [\delta]_\Sigma \qquad (5)$$

wherein $[CF_1]_\Sigma$ and $[\delta]_\Sigma$ denote the total concentrations of CF_1 and δ, respectively. The concentration of the complex $CF_1(-\delta,\epsilon)\delta^{TMR}$ is given by

$$[CF_1(-\delta,\epsilon)\delta] = [CF_1]_\Sigma\frac{[\delta]_{free}}{[\delta]_{free} + K_{d,2}} \qquad (6)$$

The simulation of the experimental data yielded a dissociation constant of the complex of $K_{d,2} = 0.8$ nM. The corresponding curve is shown in Figure 4. If a lower value for $K_{d,1}$ (dimer dissociation) is assumed, the dissociation constant for the complex has to be even smaller due to the smaller fraction of monomeric δ. The value of at least $K_{d,2} = 0.8$ nM differs greatly from the $K_d = 100$ nM that was determined by Wagner et al. (*30*). For the origin of the discrepancy, see Discussion.

Table 3: Apparent Concentrations (by FCS) of Free Dye, of Dye Bound to Subunit δ (Monomer + Dimer), and of Dye Bound through δ to $CF_1(-\delta,\epsilon)$, Respectively, as a Function of the Added Concentration of $CF_1(-\delta,\epsilon)$[a]

$[CF_1(-\delta,\epsilon)]_\Sigma$ (nM)	apparent concn of freely diffusing particles (nM)	% free dye (TMR)	% δ (monomer + dimer)	% complexed by CF_1
200	9.7	12	2	86
150	9.7	12	4	84
100	9.7	12	5	83
50	6.9	6	15	79
20	6.5	19	16	65
10	5.4	17	38	45
5	5.6	19	48	33
2	6.0	18	64	18
1	5.6	19	72	9

[a] The added concentration of TMR-labeled δ was 10 nM. The greater proportion of the dye was bound either to δ itself or through δ to $CF_1(-\delta,\epsilon)$. It was obvious that $CF_1(-\delta,\epsilon)$ monomerized the δ dimers upon binding (see second column).

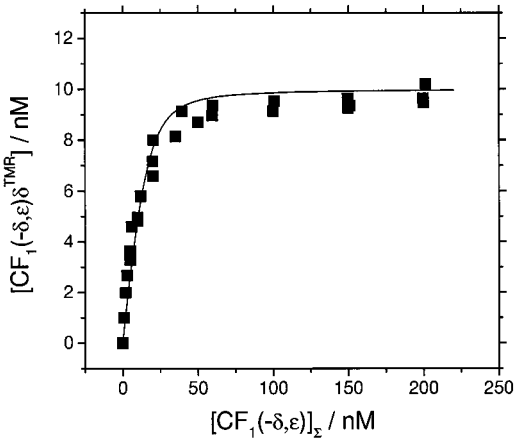

FIGURE 4: Binding of δ^{TMR} and $CF_1(-\delta,\epsilon)$ in dependence of the $CF_1(-\delta,\epsilon)$ concentration. Experiments were performed in the presence of 10 nM δ^{TMR} in Tris buffer (pH 7.8) (squares, experimental; curve calculated according to eqs 5 and 6).

Debinding of δ^{TMR} in the Presence of Unlabeled δ. These experiments were designed to inquire whether the binding constants of labeled and unlabeled δ to CF_1 differed from each other. The debinding of δ^{TMR} from $CF_1(-\delta,\epsilon)\delta^{TMR}$ was studied by the addition of unlabeled δ to displace δ^{TMR} from CF_1 in a mixture with a large overshoot of 200 nM $CF_1(-\delta,\epsilon)$ over 10 nM δ^{TMR}. When unlabeled δ was absent, almost all δ^{TMR} was bound to $CF_1(-\delta,\epsilon)$. The concentration of the complex $CF_1(-\delta,\epsilon)\delta^{TMR}$ practically equaled 10 nM (see Figure 4). Because unlabeled δ expelled labeled molecules from their binding site on CF_1, the concentration of labeled complex decreased with increasing concentration of unlabeled δ (see Figure 5A). The observed behavior was exactly as expected if the ratio of labeled to unlabeled δ on CF_1 was constant throughout, in other words, if both labeled and unlabeled δ had the same binding affinity. In these experiments we used two varieties of δ, engineered δ_{S10C} and wild-type δ. Both varieties showed the same behavior indicating the same affinity toward $CF_1(-\delta,\epsilon)$. The inserted curve in Figure 5A results from the model of two competitive reactions as introduced above (eqs 5 and 6). Because the concentration of labeled δ was much smaller than the one of unlabeled δ, $[\delta^{TMR}] \ll [\delta]_{add}$, the added amount of δ was equal to the total. The concentration of $CF_1(-\delta,\epsilon)\delta^{TMR}$ was

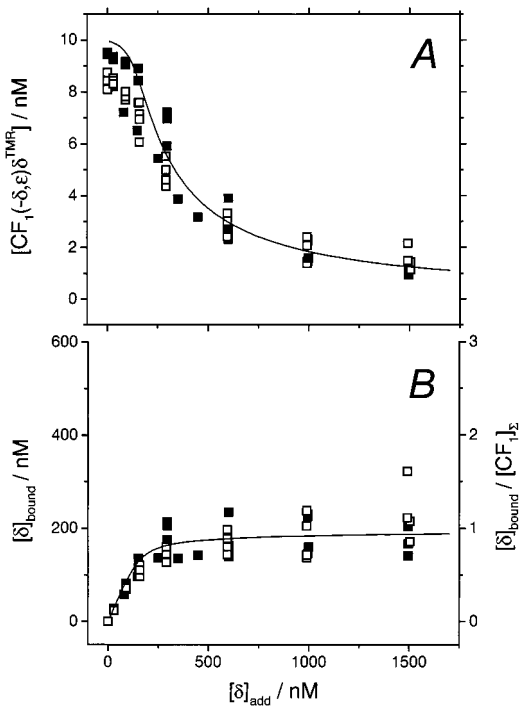

FIGURE 5: Influence of the addition of unlabeled δ_{S10C} (solid squares) and δ_{WT} (open squares) on the concentration by FCS of $CF_1(-\delta,\epsilon)\delta^{TMR}$ (A) and of bound δ (B). The experiments were performed in the presence of 200 nM $CF_1(-\delta,\epsilon)$, 10 nM δ^{TMR}, and 10 mM DTT in Tris buffer (pH 7.8). Curves are calculated with the above determined dissociation constants of the δ-dimer (0.2 nM) and the δ-containing CF_1, 0.8 nM.

then calculated from

$$[CF_1(-\delta,\epsilon)\delta^{TMR}] = [CF_1(-\delta,\epsilon)\delta]\frac{[\delta^{TMR}]_\Sigma}{[\delta]_\Sigma} \qquad (7)$$

where $[\delta^{TMR}]_\Sigma$ and $[\delta]_\Sigma$ are the total amounts of δ^{TMR} and δ, respectively. The concentration of $CF_1(-\delta,\epsilon)\delta$ was calculated from eqs 5 and 6 taking into account the same dissociation constants as above. The calculated curve fitted the experimental data (see Figure 5A). Because the concentration of labeled δ was much smaller than the one of added $CF_1(-\delta,\epsilon)$, $[\delta^{TMR}]_\Sigma \ll [CF_1(-\delta,\epsilon)]$, only one labeled δ molecule was bound to $CF_1(-\delta,\epsilon)$ at the most. Accordingly, the concentration of bound δ for different amounts of added δ was calculated from $[\delta]_{bound} = [\delta^{TMR}]_{bound}[\delta]_\Sigma/[\delta^{TMR}]_\Sigma$. The results are presented in Figure 5B. At saturating concentration of added δ, we found that the amount of bound δ equaled the concentration of $CF_1(-\delta,\epsilon)$, 200 nM. *It implied the binding of only a single copy of δ to CF_1.*

DISCUSSION

Fluorescence correlation spectroscopy (FCS) in the femtoliter volume of a laser focus is a highly sensitive tool to determine binding/dissociation equilibria in the nanomolar range. Our work demonstrated, however, that this method is prone to considerable error if not corrected for the strong effects on the size of this volume of very small alterations of the refractive index (by only 0.07%), which might be caused by adding detergents or buffers to the suspending medium.

ATP synthase is an astounding enzyme with a chemical generator, F_1, that is driven by an electrochemical motor, F_o. These two functions are mechanically coupled by a central rotor (subunits $\gamma\epsilon\mathbf{c}_{12}$) and an eccentric counter bearing (subunits $\mathbf{ab}_2\delta(\alpha\beta)_3$) as illustrated in Figure 1. The assignment of subunits to rotor and stator is based on a wealth of biochemical and biophysical evidence (see introduction). Whereas the chemical function, the synthesis of ATP, occurs at three basically equivalent reaction sites on $(\alpha\beta)_3$ in a three-stepped rotary progression (*9*, *10*, *20*) by 120° each, the progression in the electrochemical drive is probably twelve-stepped by 30° each. This is suggested by the relative abundance of the **c** subunit [namely, 12 copies per enzyme molecule (*38*)] and by the proton-over-ATP stoichiometry of four (*39*−*41*). Although not yet proven, it is rather likely that the translocation of protons (or Na^+) is sequential, as assumed in current models of the function of the electrochemical rotary drive (*5*, *13*) (overview in ref *16*). It implies that free energy derived from the translocation of four protons is transiently stored as an elastic deformation of the enzyme. It has been proposed that the intertwined helices of subunit γ might serve as a torsional spring, the two parallel helices of $\mathbf{b}_2$ as a parallelogram-shaped one (*5*), and the two segments of each subunit β as a cantilever spring (*42*). The covalent cross-linking of subunit δ to $(\alpha\beta)_3$ did not impair the (cooperative 3-site) activity of ATP hydrolysis (*18*). This observation and the fact hat the same proton-over-ATP stoichiometry has been observed both under static-head conditions (*40*, *41*) as well as far from equilibrium (*39*) can be taken as evidence for the absence of any slip of δ over its three potential binding sites on $(\alpha\beta)_3$, in other words, as evidence for its firm attachment in the unmodified holoenzyme. (For proton slip in the absence of added nucleotides, see ref *43*). Under this notion, it is to be expected that the free energy of binding to $(\alpha\beta)_3$ of subunit δ exceeds the free energy that is accumulated from the translocation of four protons or from the hydrolysis of ATP per step of 120°, namely, 50.5 kJ mol^{-1} (see introduction).

In a previous study by rotational diffusion in solution (*30*), our laboratory found a dissociation constant of 100 nM between δ and CF_1. According to the relation between K_d and the standard free energy of binding, $\Delta G° = -RT \ln K_d$, it amounts to 39.9 kJ mol^{-1}, which is less than the expectation for the stored elastic energy. It implied that δ might be stripped off from its binding site on $(\alpha\beta)_3$. It is now plausible why a low binding affinity was obtained in the previous work. The applied method, namely, rotational diffusion by photoselection of a large ensemble of solubilized protein, was not sensitive enough to detect the dimerization of unbound δ. If we had ignored the dimerization for the interpretation of the present FCS data, a much larger dissociation constant had resulted, in better agreement with the previous figure. Thus, the halved free particle number of δ in FCS as compared with the number obtained by the chemical protein assay was pivotal for the newly determined high affinity of δ for CF_1.

In the present work, a higher affinity or a lower value for K_d was determined, namely, $\leq$0.8 nM. This figure is equivalent to a standard free energy of $\geq$51.9 kJ mol^{-1} and better compatible with the notion that δ is firmly attached to $(\alpha\beta)_3$, a prerequisite for the rotary function of this enzyme.

The binding strength of δ to $CF_1(-\delta,\epsilon)$ is larger than encountered for certain ligand/receptor pairs [K_d/ligand/(ref)] [1.7 nM/angiotensin/(*44*)−4.7 nM/ferritin/(*45*)] but weaker than for the most specific antibodies [0.04 nM/ribosome/(*46*)].

Our data gave evidence for the binding of only one single copy of δ to the $(\alpha\beta)_3$ hexagon, as already found by biochemical and immunological studies (*31*). It implied that the binding of a single copy of δ breaks the structural symmetry of F_1 in a way as to prevent the binding of other copies. A first clue of how the binding of a first molecule of δ prevents the binding of further ones comes from recent electron microscopic work by Stephan Wilkens (personal communication). One portion of δ seems to cover the β-barreled top domain of F_1. The coverage might hamper the binding of a second copy of δ. It has remained enigmatic, however, why the structural symmetry breaking by δ is not paralleled by a functional symmetry breaking with regard to the rotary and cooperative catalytic mechanism of this enzyme.

ACKNOWLEDGMENT

We thank our collegues Drs. Siegfried Engelbrecht, Birgit Hecks, and Carsten Gall (the latter two at Evotec) for valuable help and discussion and Evotec/Hamburg−Zeiss/Jena for support.

REFERENCES

1. Mitchell, P. (1966) *Physiol. Rev. 41*, 445−502.
2. Laubinger, W., and Dimroth, P. (1989) *Biochemistry 28*, 7194−7198.
3. Abrahams, J. P., Leslie, A. G. W., Lutter, R., and Walker, J. E. (1994) *Nature 370*, 621−628.
4. Boyer, P. D. (1997) *Annu. Rev. Biochem. 66*, 717−749.
5. Junge, W., Lill, H., and Engelbrecht, S. (1997) *Trends Biochem. Sci. 22*, 123−456.
6. Duncan, T. M., Bulygin, V. V., Zhou, Y., Hutcheon, M. L., and Cross, R. L. (1995) *Proc. Natl. Acad. Sci. U.S.A. 92*, 10964−10968.
7. Sabbert, D., Engelbrecht, S., and Junge, W. (1996) *Nature 381*, 623−626.
8. Noji, H., Yasuda, R., Yoshida, M., and Kinosita, K. (1997) *Nature 386*, 299−302.
9. Häsler, K., Engelbrecht, S., and Junge, W. (1998) *FEBS Lett. 426*, 301−304.
10. Yasuda, R., Noji, H., Kinosita, K., and Yoshida, M. (1998) *Cell 93*, 1117−1124.
11. Zhou, Y., Duncan, T. M., and Cross, R. L. (1997) *Proc. Natl. Acad. Sci. U.S.A. 94*, 10583−10587.
12. Junge, W., Sabbert, D., and Engelbrecht, S. (1996) *Ber. Bunsen-Ges. Phys. Chem. 100*, 2014−2019.
13. Elston, T., Wang, H., and Oster, G. (1998) *Nature 391*, 510−514.
14. Vik, S. B., Patterson, A. R., and Antonio, B. J. (1998) *J. Biol. Chem. 273*, 22159.
15. Dimroth, P., Wang, H., Grabe, M., and Oster, G. (1999) *Proc. Natl. Acad. Sci. U.S.A. 96*, 4924−4928.
16. Junge, W. (1999) *Proc. Natl. Acad. Sci. U.S.A. 96*, 4735−4737.
17. Ogilvie, I., Aggeler, R., and Capaldi, R. A. (1997) *J. Biol. Chem. 272*, 16652−16656.
18. Lill, H., Hensel, F., Junge, W., and Engelbrecht, S. (1996) *J. Biol. Chem. 271*, 32737−32742.
19. Berzborn, R. J., and Finke, W. (1989) *Z. Naturforsch. 44*, 480−486.
20. Katoyamada, Y., Noji, H., Yasuda, R., Kinosita, K., and Yoshida, M. (1998) *J. Biol. Chem. 273*, 19375−19377.

21. Engelbrecht, S., and Junge, W. (1997) *FEBS Lett. 414*, 123−456.
22. Beckers, G., Berzborn, R. J., and Strotmann, H. (1992) *Biochim. Biophys. Acta 1101*, 97−104.
23. Kaim, G., and Dimroth, P. (1995) *Eur. J. Biochem. 222*, 615−623.
24. Dunn, S. D., and Chandler, J. (1998) *J. Biol. Chem. 273*, 8646−8651.
25. Mclachlin, D. T., Bestard, J. A., and Dunn, S. D. (1998) *J. Biol. Chem. 273*, 15162−15168.
26. Wilkens, S., and Capaldi, R. A. (1998) *Nature 393*, 29.
27. Boekema, E. J., Ubbing-Kok, T., Lolkema, J. S., Brisson, A., and Konings, W. N. (1997) *Proc. Natl. Acad. Sci. U.S.A. 94*, 14291−14293.
28. Pänke, O., and Rumberg, B. (1999) *Biochim. Biophys. Acta*, in press.
29. Cherepanov, D., Mulkidjanian, A., and Junge, W. (1999) *FEBS Lett. 449*, 1−6.
30. Wagner, R., Apley, E. C., Engelbrecht, S., and Junge, W. (1988) *FEBS Lett. 230*, 109−115.
31. Engelbrecht, S., Schürmann, K., and Junge, W. (1989) *Eur. J. Biochem. 179*, 117−122.
32. Engelbrecht, S., Lill, H., and Junge, W. (1986) *Eur. J. Biochem. 160*, 635−643.
33. Steinemann, D., Lill, H., Junge, W., and Engelbrecht, S. (1994) *Biochim. Biophys. Acta 1187*, 354−359.
34. Sedmark, J. J., and Grossberg, S. E. (1994) *Anal. Biochem. 79*, 544−552.
35. Elson, E., and Magde, D. (1974) *Biopolymers 13*, 1−27.
36. Aragón, S. R., and Pecora, R. (1976) *J. Chem. Phys. 64*, 1791−1803.
37. Rigler, R., Widengren, J., and Mets, U. (1992) in *Fluorescence spectroscopy* (Wolfbeis, O. S., Ed.) pp 13−24, Springer-Verlag, New York.
38. Jones, P. C., Jiang, W. P., and Fillingame, R. H. (1998) *J. Biol. Chem. 273*, 17178−17185.
39. Berry, S., and Rumberg, B. (1996) *Biochim. Biophys. Acta 1276*, 51−56.
40. van Walraven, H. S., Strotmann, H., Schwarz, O., and Rumberg, B. (1996) *FEBS Lett. 379*, 309−313.
41. Pänke, O., and Rumberg, B. (1997) *Biochim. Biophys. Acta 1322*, 183−194.
42. Shirakihara, Y., Leslie, A. G. W., Abrahams, J. P., Walker, J. E., Ueda, T., Sekimoto, Y., Kambara, M., Saika, K., Kagawa, Y., and Yoshida, M. (1997) *Structure 5*, 825−836.
43. Groth, G., and Junge, W. (1993) *Biochemistry 32*, 8103−8111.
44. Ishida, J. J., Asada, S., Daitoku, H., Fujiwara, K., Kon, Y., Sugaya, T., Murakami, K., Nakajima, T., Kasuya, Y., and Fukamizu, A. (1999) *Int. J. Mol. Med. 3*, 263−270.
45. Hulet, S. W., Hess, E. J., Debinski, W., Arosio, P., Bruce, K., Powers, S., and Connor, J. R. (1999) *J. Neurochem. 72*, 868−874.
46. Hanes, J., Jermutus, L., Weber-Bornhauser, S., Bosshard, H. R., and Pluckthun, A. (1998) *Proc. Natl. Acad. Sci. U.S.A. 95*, 14130−14135.

BI991236M